©CSIRO 2010 *Environ. Chem.* **2010**, *7*, 377–385. doi:10.1071/EN10003_AC

Accessory publication

Characterisation of structural and surface speciation of representative commercially available cerium oxide nanoparticles

M. Baalousha,[A,D] *P. Le Coustumer*,[B] *I. Jones*[C] *and J. R. Lead*[A]

[A]School of Geography, Earth and Environmental Sciences, University of Birmingham, Edgbaston, B15 2TT, UK.

[B]Université de Bordeaux, B.18 av Facultés, F-33405 Talence, France.

[C]School of Metallurgy and Materials, University of Birmingham, Edgbaston, B15 2TT, UK.

[D]Corresponding author. Email: m.a.baalousha@bham.ac.uk

Materials and methods

HR-TEM-EELS

Each electron loss near edge structure (ELNES) is characterised by a steep rise near the energy of the white lines. This intensity is due to transition of a core electron to an unbound state and is very high relative to the overall intensity of the ELNES spectrum. However, the ELNES spectrum also contains an exponentially decaying background due to the tail of the strong zero loss peak, plural scattering depending on sample thickness and a contribution from the transitions to the atomic continuum.[1] In order to analyse the PEELS spectra quantitatively, the data were treated by a series of operations in order to reduce them to their structure-dependent components by removing the previously mentioned features as described in Garvie and Buseck,[2] Yang and Mobus,[3] and Zhang et al [4] and described below and shown in Figs A1 and A2.

Peak area evaluation method

- All spectra were corrected for dark current and gain variation of the parallel detector using a dark count spectrum for every sample spectrum (or series of spectra) and a gain normalisation spectrum for each EELS session.
- Then the background intensity at the Ce M_{4-5} edge was subtracted by fitting an inverse power-law of the form AR^{-r} for a range of 20–30 eV before the edge and extrapolating this function to higher energies and this background was subtracted.
- The multiple inelastic scattering effects (Egerton[5]; Ahn[6]) in the core-loss region were removed using the low-loss spectrum and the Fourier ratio routine of the EL/P package. Consequently, the data presented here are the result of single scattering processes. These processes were performed with the Gatan el/p 3.0 PEELS software.

- The remainder of the spectrum was fitted analytically in order to remove the contribution from the transitions to the atomic continuum. This feature was regarded as a double arctan functions with inflection points located near the white lines

$$f(\Delta E) = \frac{h_1}{180}\left[\arctan\left(\frac{180}{w_1}\cdot(\Delta E - E_1)\right)\cdot\frac{180}{\pi} + 90\right] + \frac{(h_2 - h_1)}{\pi}\left[\arctan\left(\frac{180}{w_2}\cdot(\Delta E - E_2)\right)\cdot\frac{180}{\pi} + 90\right] \quad (1)$$

where the two arctan functions were constrained to zero at low energies and step height (h_1 and h_2) are scaled to the minima behind M_5 and M_4 white lines respectively, position of inflection points E1 and E2 corresponding to the white lines respectively and a slope *w*.

- Then the area under the M_5 and M_4 peaks were calculated and used to calculate the fraction of Ce^{3+} or Ce^{4+} contained in the particles applying Eqn 2

$$Ce^{4+} = 1 - \frac{(M_5/M_4)_{Ce^{4+}} - (M_5/M_4)_{Particle}}{(M_5/M_4)_{Ce^{4+}} - (M_5/M_4)_{Ce^{3+}}} \quad (2)$$

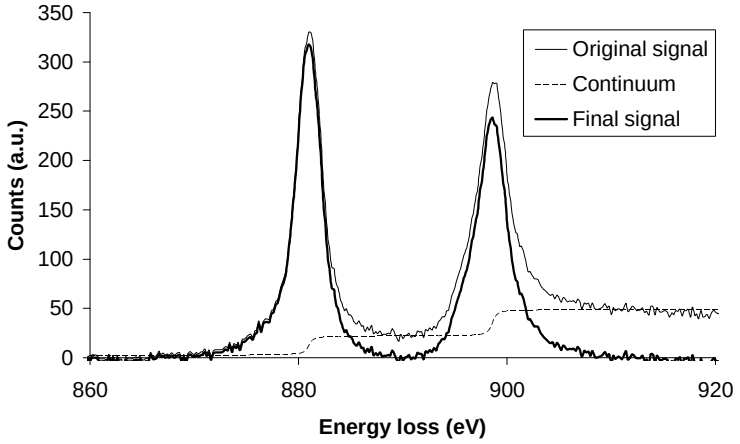

Fig. A1. Typical electron energy loss spectroscopy spectra of Ce^{III} standard, illustrating spectrum analysis procedure by area evaluation method.

2nd derivative method

After the removal of the background and the multiple electron scattering as described above, the 2nd derivative was calculated numerically using EL/P software. The 2nd derivative is useful particularly when dealing with sharp 'white lines' as the choice of the window over which to integrate the peak area is essentially automatic; one can take the positive area between the zero crossings as marked by the shaded area in Fig. A2.

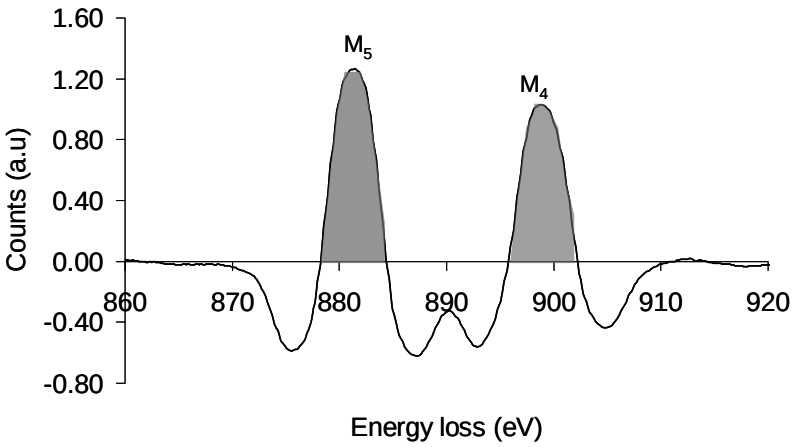

Fig. A2. Typical electron energy loss spectroscopy spectra of Ce^{III} standard, illustrating spectrum analysis procedure by second derivative.

Origin of the white lines for cerium

The M_{54} edges reflect the transition of 3d core electrons to unoccupied states of p-like and f-like symmetry. The dipole allowed transitions $3d^{10}4f^{n} \rightarrow 3d^{9}4f^{n+1}$ are responsible for the occurrence of the white lines $M_{5,4}$, which are characteristic of the *4f*-shell occupancy of the excited ion. These transitions mask the much weaker 3d→p edge. The $M_{5,4}$ edges arises from the two ways in which the spin quantum number, *s*, couples to the orbital quantum number, *l*, giving a total angular momentum, $j = l+s$. This coupling results in two peaks: M_5 corresponds to transitions from the $3d_{5/2}$ (j = 5/2) and M_4 from the $3d_{3/2}$ (j = 3/2) level. The energy difference $\Delta(M_5–M_4)$ is a measurement of the spin-orbit splitting of the 3d level and is ~18.0 eV for cerium.

Morphology and crystal structure

The crystal structure of cerium oxide is that of the fluorite (CaF_2) structure.[4] The unit cell of CeO_2 is made of a face centred cubic structured Ce lattice with a cubic oxygen cage located at the tetrahedral matrices. The crystal lattice of cerium oxide is shown in Fig. A3a and the projection of the crystal structure along the <110> direction is shown in Fig. A3b, which shows the different atomic planes that can be observed along the <110> direction, along with the distances and angles between the atomic planes as observed in the <110> projection. Fig. A4 shows the different possibilities of the surface atomic planes (low index) that can surround the particles, the distances and angles between the different atomic planes and the corresponding morphology of each particle. There are four different possibilities, which are: (i) a rhombus projection terminated by four {111} atomic planes and corresponding to a tetrahedral morphology terminated by eight {111} planes; (ii) a hexagonal projection terminated by four {111} atomic planes and two {002} atomic planes and corresponds to a truncated octahedral terminated by eight {111} and two {002} facets; (iii) a hexagonal projection terminated by four {111} atomic planes and two {220} atomic planes and corresponds to a truncated octahedral terminated by eight {111} and four {220} facets; and (iv) an octagonal projection terminated by four {111}, two {220} and two {002} atomic planes and corresponds to a truncated octahedral morphology terminated by eight

{111}, two {002} and four {220} facets. Determining the distances and angles between the atomic planes allows identifying the crystal structure and particle morphology, and this is investigated here by HR-TEM.

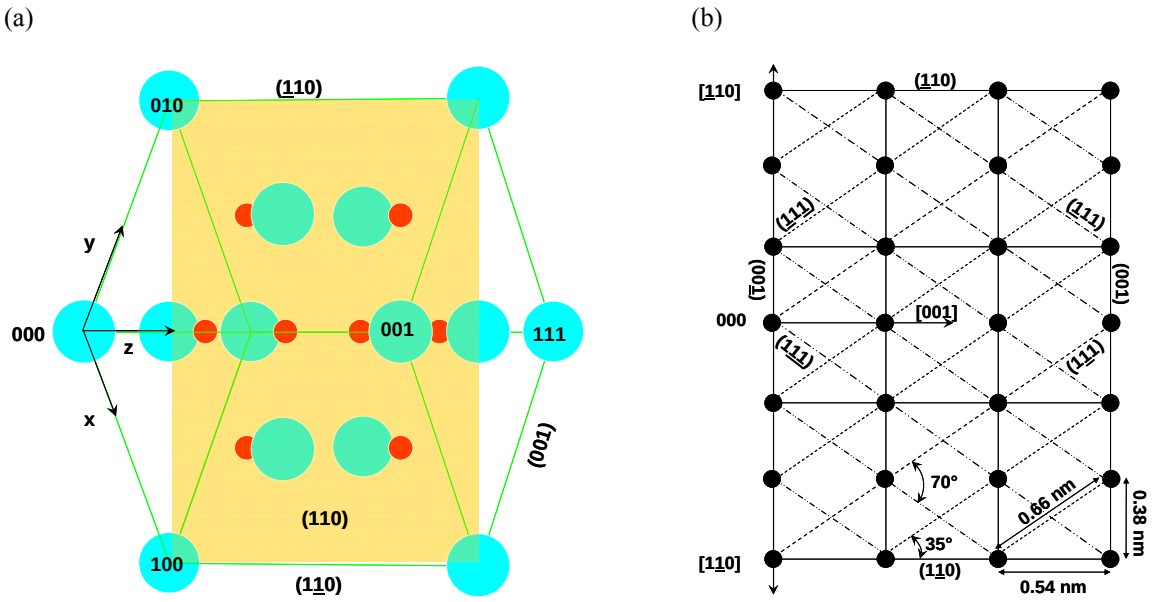

Fig. A3. (a) Crystal lattice of cerium oxide, where large spheres represent cerium atoms while small spheres represent oxygen atoms. (b) A projection of the cerium oxide lattice along the <110> direction with the different atomic planes that can be observed.

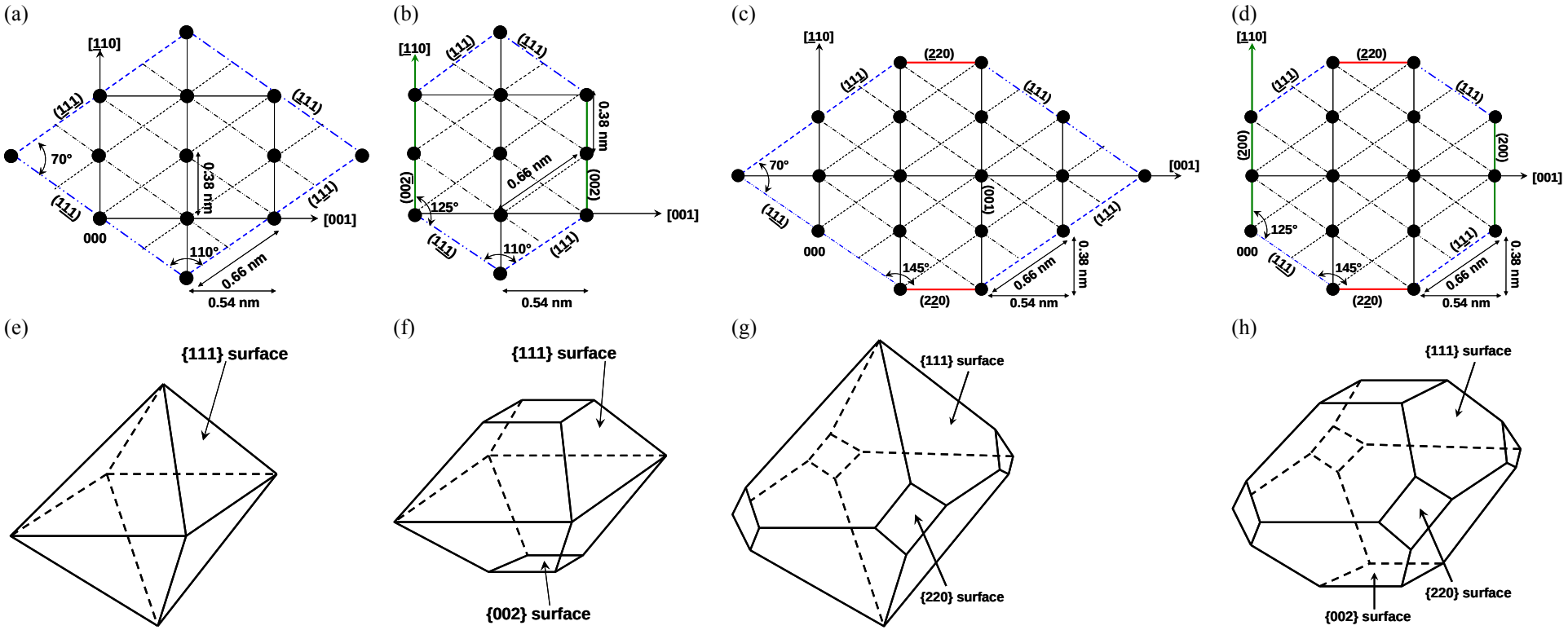

1 **Fig. A4.** A projection along the <110> direction of a particle limited by: (a) four {111} atomic planes; (b) four {111} and two {002} atomic planes; (c) four
2 {111} and two {220} atomic planes; (d) four {111}, two {002} and two {220} atomic planes. (e–h) Schematic geometry of ceria NP corresponding to the
3 projections in (a–d).

Thickness of the Ce^{3+} layer

The thickness of the Ce^{3+} layer can be calculated according to Eqn 3 assuming that each particle consist of a thin surface layer of Ce_2O_3 as described in Wu et al.[7] and data are presented in Fig. A5.

$$\Delta d = 0.5d\left[1-\left(1-f_v\right)^{1/3}\right] \quad (3)$$

where d is the diameter of the particles and f_v is the volume fraction of Ce_2O_3 calculated by Eqn 2.

Clearly, the thickness of Ce^{III} decreases with the decreased proportion of the Ce^{III}, with the highest value for the nanoparticles (2.9 ± 2.9 nm, or 2.3 ± 1.0 nm, depending on EELS data analysis method), which decreases after interaction with humic substance or biological media and tends to disappear for the bulk particles.

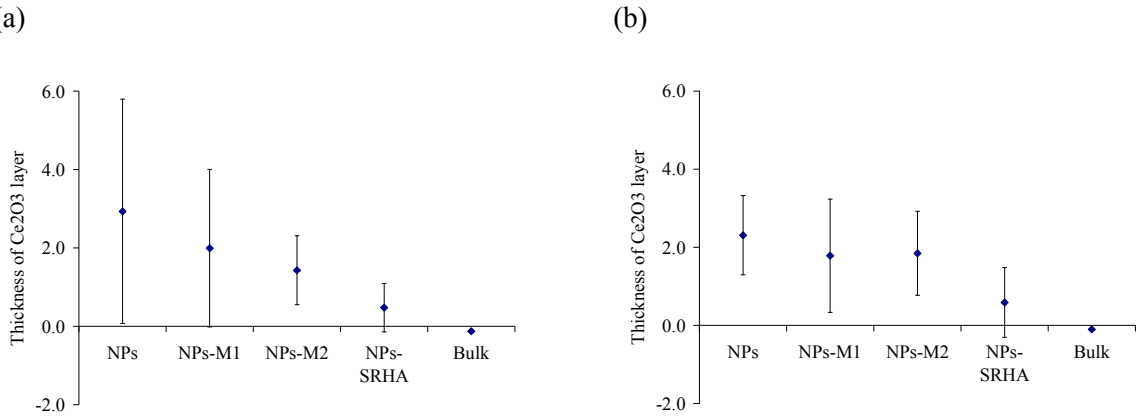

Fig. A5. The calculated thickness of Ce_2O_3 surface layer (nm) for ceria NPs in $NaNO_3$ and the different media (b) based on the data presented in Fig. 4b and (b) based on the data presented in Fig. 4c. SRHA, Suwannee River humic acid; M1, algal biological media+buffer; and M2, biological media (M2279) used to grow C3A human hypatocyte cells.

References

[1] D. B. Williams, C. B. Carter, *Transmission Electron Microscopy: Spectroscopy* **1996** (Springer: New York).

[2] L. A. J. Garvie, P. R. Buseck, Determination of Ce^{4+}/Ce^{3+} in electron-beam-damaged CeO_2 by electron energy-loss spectroscopy. *J. Phys. Chem. Solids* **1999**, *60*, 1943. doi:10.1016/S0022-3697(99)00218-8

[3] G. Yang, G. Mobus, R. Hand, Fine structure EELS analysis of glasses and glass composites. *J. Physics. Conf. Series* **2006**, *26*, 73. doi:10.1088/1742-6596/26/1/017

[4] F. Zhang, Q. Jin, S.-W. Chan, Ceria nanoparticles: size, size distribution, and shape. *J. Appl. Phys.* **2004**, *95*, 4319. doi:10.1063/1.1667251

[5] R. Egerton. *Electron Energy-loss Spectroscopy in the Electron Microscope, Second edn* **1996** (Plenum Press: New York).

[6] C. C. Ahn, *Transmission Electron Energy Loss Spectrometry in Materials Science and the EELS Atlas, Second edn* **2004** (Wiley-VCH Verlag: Weinheim).

[7] L. Wu, H. J. Wiesmann, A. R. Moodenbaugh, P. F. Klie, Y. Zhu, D. O. Welch, M. Suenaga, Oxidation state and lattice expansion of CeO_{2-x} nanoparticles as a function of particle size. *Phys. Rev. B* **2004**, *69*, 125415. doi:10.1103/PhysRevB.69.125415